UDC 578.23: 578.76: 615.281.8 doi: https://doi.org/10.15407/ubj94.03.081

DECAMETHOXIN VIRUCIDAL ACTIVITY: *IN VITRO* AND *IN SILICO* STUDIES

I. V. SEMENYUTA[1]✉, O. P. TROKHIMENKO[2], I. V. DZIUBLYK[2], S. O. SOLOVIOV[2,3], V. V. TROKHYMCHUK[2], O. L. BORODOVA[4], D. M. HODYNA[1], M. P. SMETIUKH[3], O. K. YAKOVENKO[5], L. O. METELYTSIA[1]

[1]*V. P. Kukhar Institute of Bioorganic Chemistry and Petrochemistry, National Academy of Sciences of Ukraine, Kyiv;*
[2]*Shupyk National Healthcare University of Ukraine, Kyiv;*
[3]*National Technical University of Ukraine "Igor Sikorsky Kyiv Polytechnic Institute", Kyiv;*
[4]*F. G. Yanovsky Institute of Tuberculosis and Pulmonology, National Academy of Medical Sciences of Ukraine, Kyiv;*
[5]*Volyn Regional Clinical Hospital, Lutsk, Ukraine;*
✉*e-mail: ivan@bpci.kiev.ua*

Received: 09 June 2021; **Revised:** 11 September 2022; **Accepted:** 29 September 2022

The data on the representative of decamethoxin short-term action on infectious bronchitis virus (IBV) strain H120 used as a human-safe model of SARS-CoV-2 virus are presented. The viral activity was estimated with the use of inverted microscope PrimoVert (Germany) by destructive effect on BHK21 fibroblastic cell line. In vitro results demonstrated that decamethoxin (100 μg/ml) completely inactivated IBV coronavirus strain at exposure of 30 sec and more. At the lowest decamethoxin exposure of 10 sec the antiseptic virucidal activity was 33% and 36% of control at 24 and 48 h of cultivation respectively. Molecular docking analysis indicated the significant similarity of IBV and SARS-CoV-2 main protease (M^{pro}) structure. Docking studies of decamethoxin interaction with IBV M^{pro} and SARS-CoV-2 M^{pro} active centers demonstrated the ligand-protein complexes formation with the estimated binding energy of -8.6, -8.4 kcal/mol and key amino acid residues ASN26, GLY141, GLU187, GLU164, THR24, THR25, ASN142, GLY143, CYS145, HIS164 and GLU166.

K e y w o r d s: decamethoxin, QAC, virucidal activity, IBV strain H120, SARS-CoV-2, main protease, molecular docking.

Disinfectants and antiseptics are important determinants in a pandemic, including coronavirus infection (COVID-19). Successful disinfection of SARS-CoV-2 is defined by the characteristics of the virus, the properties of the disinfectant or antiseptic, and the environmental conditions in which the virus is present. SARS-CoV-2 is stable over a wide pH range (pH 3–10) at room temperature [1] and is very stable in a favorable environment [2] but is usually disinfected [3]. Considering viral load, persistence, stability, viability and environmental factors, disinfection of medical and other public facilities is a necessary part to prevent transmission and waves of COVID-19 infection.

Among the well-known disinfectants such as detergents, acids, oxidizing agents, alcohols, alkalis, aldehydes, biguanides, halogens, phenols, quaternary ammonium compounds (QAC) occupy a special place [4]. Most disinfectants target the outer lipid layer of coronaviruses [5]. Cross-linking, coagulation, structural and functional damage and oxidation appear to be the main mechanisms of the disinfectants virucidal activity [6]. In the case of coronaviruses, disinfectants affect the protein and lipid structures of the coronavirus and limit the spread of the virus [7].

Quaternary ammonium compounds (QACs) as cationic surfactants contain the amphiphilic molecules and have a broad spectrum of antimicrobial activity [8]. Their chemical structure includes four aliphatic or aromatic radicals linked to a central nitrogen atom. The antibacterial and antifungal activity of QAC is associated with the presence of 12 to 16 carbon atoms in their alkyl chain [9].

Wherein, the antimicrobial mechanism of QAC action is based on the electrostatic interaction of a positively charged cationic element of QAC with a

negative charge of the cytoplasmic membrane of bacteria or fungi, leading to membrane disorganization and its autolysis. In the case of SARS-CoV-2, disruption of the phospholipid bilayer by QAC occurs more easily due to the lack of a cell wall in the virus [10].

The basic/cationic structure of QAC is a quaternary nitrogen fragment (Fig. 1), which plays an important biological role in the living systems [11].

The negatively charged anionic moiety (X-) is usually chlorine or bromine and is bonded to nitrogen to form the QAC salt. This structural diversity makes it possible to significantly change/improve the QACs efficiency of and expand the scope of application including the viral infections [12]. The existing variety of QACs structural features allows to classify them into several subclasses: mono-, bis-, multi- and polyderivatives according to the number of the charged nitrogen atoms, including in heterocyclic compounds (piperidine, pyridine, imidazole, etc.) [13].

Since the beginning of the 20th century, a significant amount of work has been devoted to the development of this class of biocides. Thus, according to modern literature, since 2021 more than 17000 articles about QACs were published [14]. Virucidal activity of QACs, including anti-SARS-CoV-2 activity of decamethoxin, confirmed by a number of authors and has the scientific and practical interest in a wide range of researchers, especially in terms of potential molecular mechanisms of their virucidal action [15-21].

Today, a number of viral proteins have been established as the main targets for SARS-CoV-2 in-

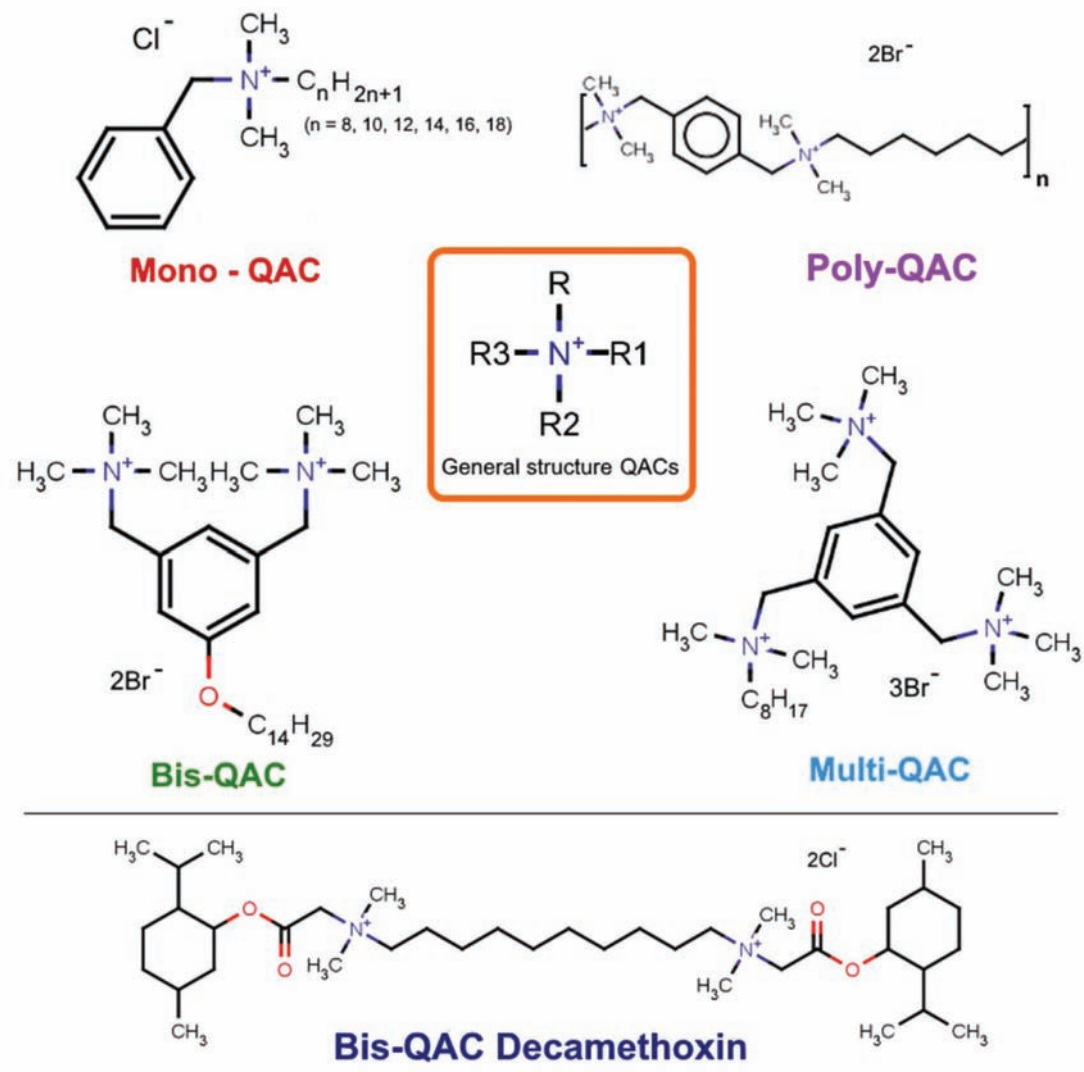

Fig. 1. Structural features of decamethoxin and QACs

hibitors, which include the spike S-protein, RNA-depleted RNA polymerase (RdRp) and main protease (M^{pro}). M^{pro} presented in many strains is a key enzyme in the coronavirus replication mechanism and is responsible for copying and reproducing the SARS-CoV-2 genetic material. Therefore, pharmacists often consider the M^{pro} as the main target in the fight against SARS-CoV-2, because its blocking can be an effective approach to preventing virus replication. In addition, M^{pro} is being intensively pursued as a main target not only for SARS-CoV-2, but also for SARS-CoV and MERS-CoV, as well as enteroviruses, rhinoviruses and noroviruses [22, 23].

Cysteine protease M^{pro} is virus encoded and contains a glutamine residue at position P1 [24]. This structural feature is absent in the related host proteases, indicating the high selectivity of M^{pro} as a target. [25].

A characteristic structure feature of the M^{pro} inhibitors is the presence of reactive functional groups (β-ketoamide, aldehyde, aldehyde bisulfite, Michael acceptors), forming the covalent bonds with the Cys145 residue in the catalytic center of the enzyme [26].

The currently known M^{pro} inhibitors - calpain II and calpain XII (are in preclinical studies) [26], as well as Boceprevir (approved as an antiviral drug) are expensive. Therefore, the search and study of new protease inhibitors seems to be an actual task.

In this regard, calculation /computational methods as well as *in vitro* methods are of particular importance, which allows one to effectively analyze the potential mechanisms of molecular interactions of promising biologically active molecules [27-30].

This paper presents the *in vitro* and *in silico* studies results of the decamethoxin virucidal activity as a representative of bis-QAC compounds.

Materials and Methods

In vitro study materials and methods. Antiseptic Dekasan (Yuria-Farm, Ukraine) with decamethoxin content of 0.2 mg was used as QAC. Non-pathogenic to human the strain H-120 virus IBV with an infectious titer by 3.0 lg $TCID_{50}$/0.1 ml was used [31].

As cell culture was used a transplant culture of BHK-21 cells obtained from the cell cultures collection of R.E. Kavetsky Institute of Experimental Pathology, Oncology and Radiology of National Academy of Sciences of Ukraine. The RPMI-1640 and DMEM mediums with low glucose and glutamine and fetal blood sera of cows (Sigma, USA) were used. Cell Proliferation Kit I (MTT) (Roche Diagnostics, Germany) was used for cell viability analysis by colorimetric method.

The volume of the cell monolayer was 100 μl. The study was conducted fourfold. Standart culture flasks (Nunc, Denmark) for 96 wells microplates with an adhesive surface (Cellstar Greiner Bio-One, Austria) were used as laboratory equipment. Inverted microscope PrimoVert (Karl Zeiss, Germany) with a video camera and compatible software was used for *in vitro* cell culture monolayer fixation and visualization of microscopy results.

In silico study materials and methods. The crystal structures of the IBV and SARS-CoV-2 main proteases are obtained from the RCSB Protein Data Bank PDB ID:2Q6F [32] and PDB ID: 7L0D [33]. The enzyme has been prepared by AutoDock Tools (ADT) 1.5.6 [34] and saved in PDBQT format. The structure of decamethoxin was created and saved in Mol format using ChemAxon Marvin Sketch 5.3.735 [35]. The structure of decamethoxin was optimized and the energy was minimized by the MOPAC2016 program [36]. For the main proteases and decamethoxin were computed of partial charges using ADT and the Gasteiger method and saved in PDBQT format. AutoDock Vina 1.1.2 [37] program was applied for the molecular docking. The docking center has been set with coordinates x = 24.017; y = -63.765; z = 10.463 and the grid map 30*30*30 points with a grid spacing of 1 Å. The presentation of the results and the ligand-protein complex analysis were conducted by Accelrys DS [38]. The N3 inhibitor was used as a co-crystal structure in the active site of the main IBV protease [39].

Results and Discussion

In vitro study. Table presents the *in vitro* study results of decamethoxin virucidal activity under the conditions of an extended time experiment based on some previously obtained data [40].

The presented *in vitro* results (Table) show that decametoxin completely inactivates IBV virus in BHK21 cell culture starting from 30 sec of exposure. At the same time, under the conditions of the lowest decamethoxin exposure (10 and 20 sec) a partial virucidal activity of the antiseptic is observed as 1 and 2 lg ($TCID_{50}$/0.1 ml) at 24 and 48 h of cultivation, respectively. At the same time (without decamethoxin treatment) the control IBV infectious titer was 4.5 and 5.5 lg ($TCID_{50}$/0.1 ml at 24 and 48 h of cultivation respectively (Fig. 2).

T a b l e. Virucidal activity of decamethoxine

Type of study samples	Decamethoxin exposure time, sec	IBV infect. titer (lg($TCID_{50}$/0.1 ml), at different cultivation times of the studied samples, h	
		24 h	48 h
BHK21-IBV (control) (1)	–	4.5	5.5
BHK21-IBV-DMX (2)	10	1.5	2.0
BHK21-IBV-DMX (3)	20	1.0	1.5
BHK21-IBV-DMX (4)	30	<0.5	<0.5
BHK21-IBV-DMX (5)	60	<0.5	<0.5
BHK21-IBV-DMX (6)	120	<0.5	<0.5
BHK21-IBV-DMX (7)	1800	<0.5	<0.5

Fig. 3 - 5 demonstrated the results of the microscopic study of the decamethoxin virucidal activity.

Thus, microscopic analysis (Fig. 3-5) of the studied samples confirmed the *in vitro* results of decamethoxin action after 30 sec exposure as the complete inactivation of IBV in BNK-21 cell culture.

In silico study. Redocking of N3 ligand into the IBV M^{pro} active site was used for the validation of the docking results. The obtained ligand-protein complex showed the estimated binding energy of -8.8 kcal/mol. Fig. 6 displays the placement of the N3 co-crystal inhibitor and docking position decamethoxin into the active site IBV M^{pro}. Also, decamethoxin and N3 inhibitor binding and localization in the IBV M^{pro} active site are similar. And amino acids ASN26, GLY141, GLU187, GLU164, ALA140, CYS143, HIS161 and PRO166 are the key in complexation.

Further, IBV M^{pro} substrate-binding site was used for the docking procedure based on the structural analysis data. Visual demonstration of the molecular docking and intermolecular interactions of decamethoxin are presented in Fig. 7.

The docking results show that the formation of the ligand-protein complex (Fig. 7) was accompanied by an estimated binding energy of -8.6 kcal/mol. This ligand-protein complex is stabilized by the six hydrogen bonds (2.22–3.66 Å) with amino acids

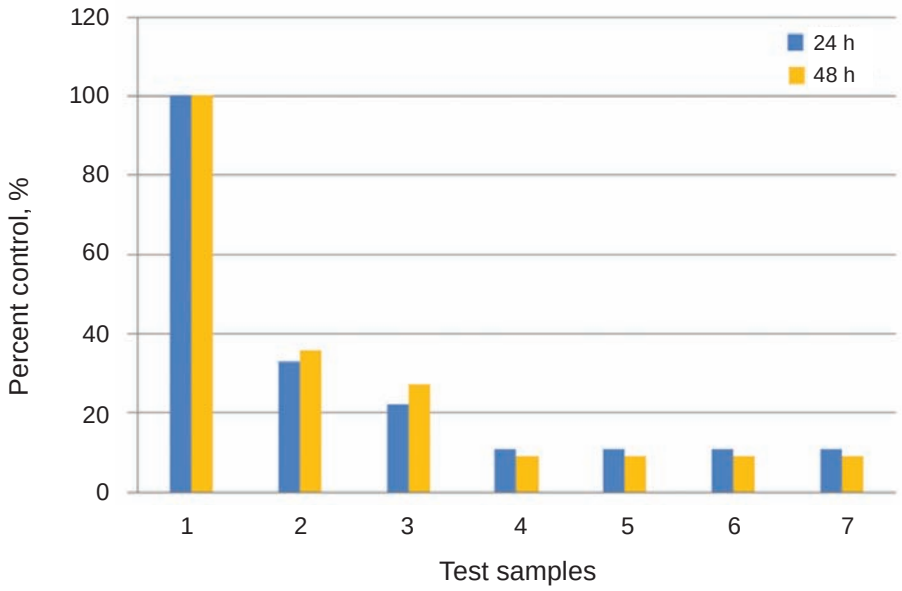

Fig. 2. Comparative analysis of in vitro virucidal activity results of decamethoxin under various experimental conditions, percent to control

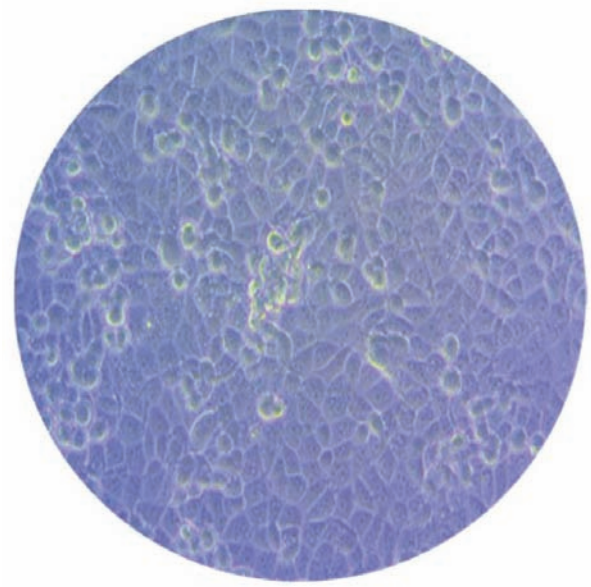

Fig. 3. BHK-21 cell culture without decamethoxin treatment (control)

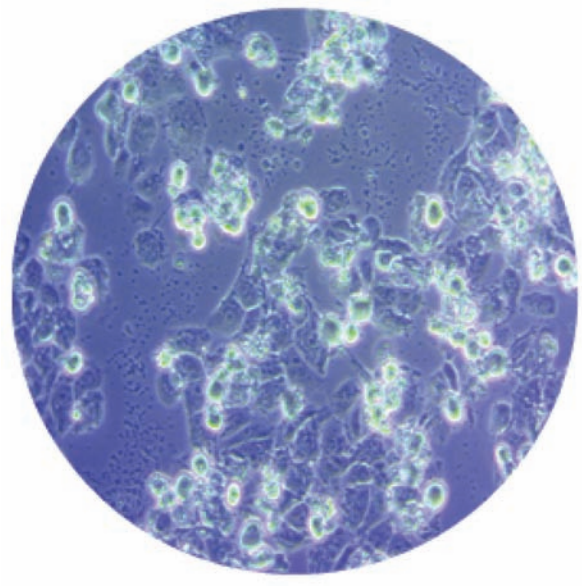

Fig. 4. Destructive changes of BHK-21 cell culture after IBV infection

ASN26, GLY141, GLU187 and GLU164, the one electrostatic interaction (3.75 Å) with GLU187 and the five hydrophobic interactions (3.87–5.19 Å) with the amino acid residues ALA140, CYS143, HIS161 and PRO166.

Sequences alignment. To confirm the potential complexation of decamethoxin in the SARS-CoV-2 M^{pro} active site, a comparative analysis (Fig. 8) of the primary structures of IBV M^{pro} (2Q6F) and SARS-CoV-2 M^{pro} (7C8B) [41] was performed using the NCBI Protein BLAST server [42].

The received results (Fig. 8) indicate the significant similarity of M^{pro} IBV and M^{pro} SARS-CoV-2 - sequence identities and sequence similarity indicators were calculated as 41 and 55%, respectively.

The M^{pro} active sites of IBV and SARS-CoV-2 were compared using the Universal Protein Resource (UniProt) the "Align" tool for multiple sequence alignment (Fig. 9) [43].

Fig. 8 as well as Fig. 9 demonstrates not only a high degree of studied enzymes similarity, but also the structural similarity of their active centers. Next, molecular docking of decamethoxin into the active site of the M^{pro} SARS-CoV-2 was performed.

The docking results demonstrate the formation of the ligand-protein complex (Fig. 10) by the estimated binding energy of -8.4 kcal/mol. This ligand-protein complex is stabilized by the seven hydrogen bonds (1.94–3.68 Å) with amino acids THR24, THR25, ASN142, GLY143, CYS145, HIS164, GLU166, the one electrostatic interaction (4.84 Å) with HIS41 and the five hydrophobic interactions (3.81–4.81 Å) with the amino acid residues HIS41, CYS145, HIS163. It is necessary to emphasize the formation of hydrogen, electrostatic and hydrophobic bonds between decamethoxine and amino acids of the catalytic dyad HIS41 - CYS145 of the M^{pro} active site.

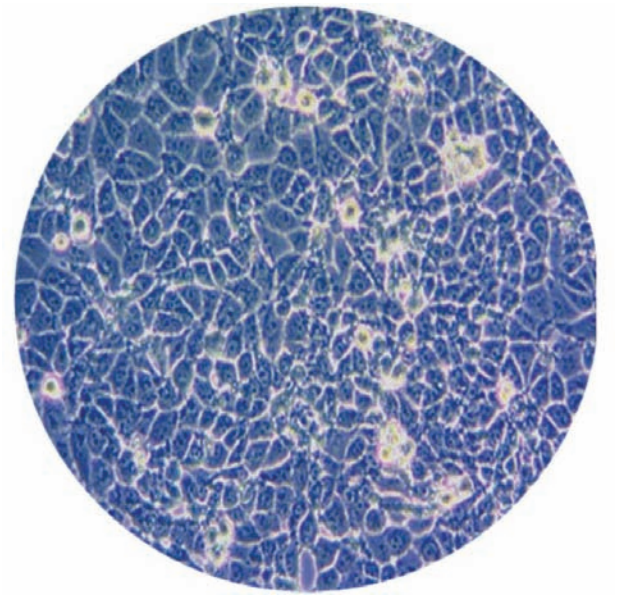

Fig. 5. BHK-21 cell culture after decamethoxin treatment (30 sec exposure)

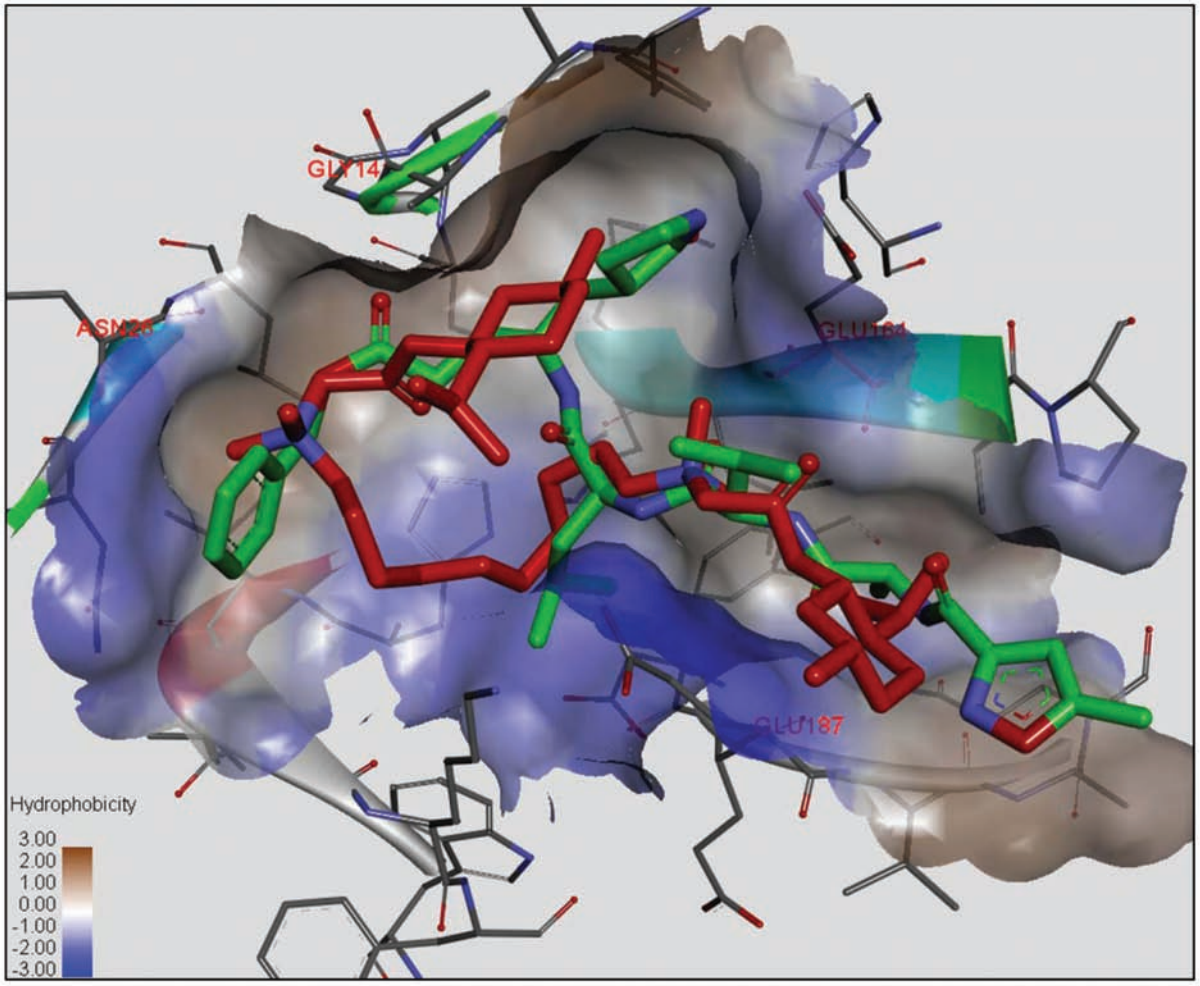

Fig. 6. Localization of N3 inhibitor and decamethoxin into the active site IBV M^{pro}; green – N3 inhibitor; red – decamethoxin

Thus, the IBV virus is used as a human-safe model of SARS-CoV-2 virus included in the single family Coronaviridae with a similar difficult structure, similar target cells, a similar pathology type and an immunological reactivity, allowing us to assume the presence of similar molecular targets for the decamethoxin action. The calculated indicators of the interactions of decamethoxin in the IBV M^{pro} and SARS-CoV-2 M^{pro} active centers can significantly expand the possibilities of searching and analyzing of new antiviral agents of various chemical classes as M^{pro} inhibitors of the SARS-CoV-2 virus.

Conclusion. Thus, obtained *in vitro* results demonstrated that decamethoxine in concentrations of 100 μg/ml completely inactivate IBV coronavirus strain for 30 sec or more. At the same time, under the conditions of the lowest decamethoxin exposure of 10 sec a partial virucidal activity of the antiseptic is observed as 1.5 and 2.0 lg ($TCID_{50}$/0.1 ml) at 24 and 48 h of cultivation, respectively. Decamethoxin virucidal properties against IBV coronavirus allow recommended as an antiseptic for non-specific prevention of coronavirus infection in adults with contact for 30 sec or more. Molecular docking studies of the potential mechanism of action have shown the complexation of decamethoxin into the active sites IBV M^{pro} and SARS-CoV-2 M^{pro}. The estimated binding energy of ligand-protein complexes M^{pro} IBV and M^{pro} SARS-CoV-2 is similar and amounts to -8.6 and -8.3 kcal/mol respectively. The amino acid residues ASN26, GLY141, GLU187, GLU164, THR24, THR25, ASN142, GLY143, CYS145, HIS164, GLU166 play a key role in the ligand-protein complex formation. The calculated high structure similarity between the M^{pro} IBV and M^{pro} SARS-CoV-2 can serve the perspective approach for the *in vitro*

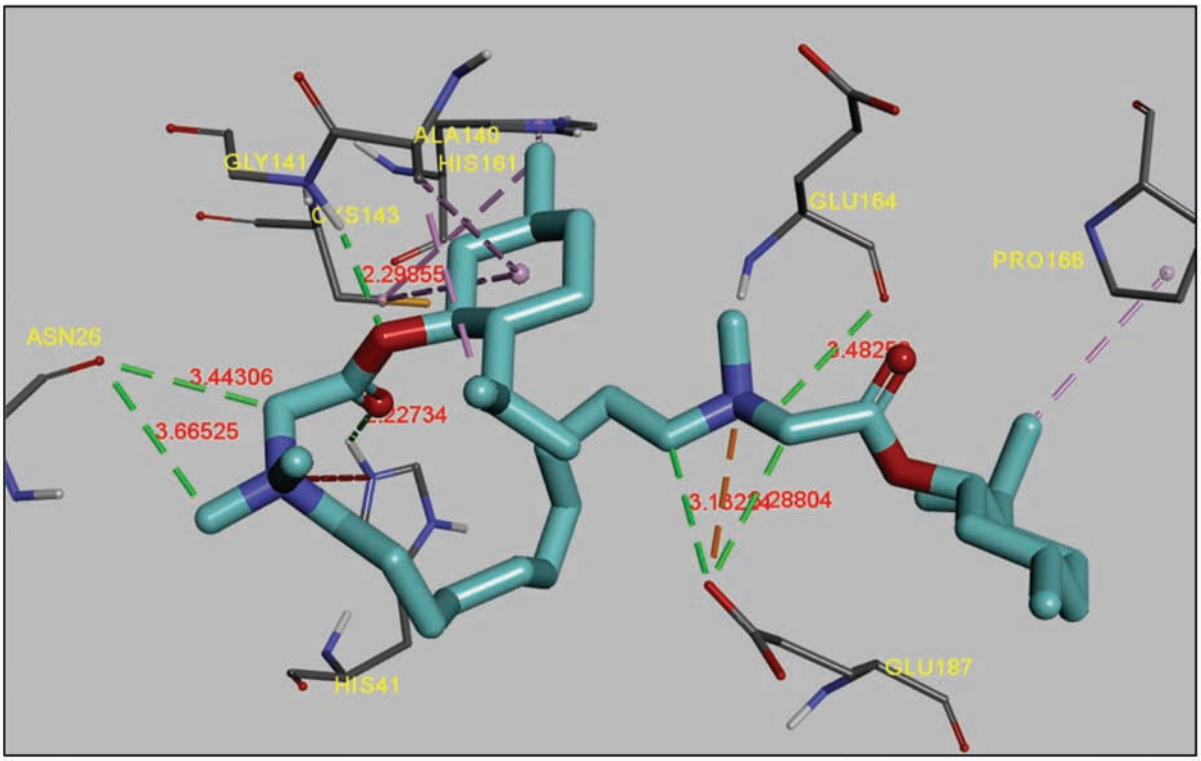

Fig. 7. Docking of decamethoxin into the IBV M^{pro} active site

Score	Expect	Method	Identities	Positives	Gaps
228 bits(580)	5e-78	Compositional matrix adjust.	129/316(41%)	175/316(55%)	19/316(6%)

```
Query  1    SGFRKMAFPSGKVEGCMVQVTCGTTTLNGLWLDDVVYCPRHVICTSEDMLNPNYEDLLIR  60
            SGF+K+  PS  VE C+V V+      LNGLWL D +YCPRHV+           + D+L
Sbjct  3    SGFKKLVSPSSAVEKCIVSVSYRGNNLNGLWLGDSIYCPRHVLG---KFSGDQWGDVLNL  59

Query  61   KSNHNFLVQAGN-VQLRVIGHSMQNCVLKLKVDTANPKTPKYKFVRIQPGQTFSVLACYN  119
             +NH F V    N V L V+    ++  VL L+    AN +TPKYKFV+    G +F++    Y
Sbjct  60   ANNHEFEVVTQNGVTLNVVSRRLKGAVLILQTAVANAETPKYKFVKANCGDSFTIACSYG  119

Query  120  GSPSGVYQCAMRPNFTIKGSFLNGSCGSVGFNIDYDCVSFCYMHHMELPTGVHAGTDLEG  179
            G+  G+Y   MR N TI+ SFL G+CGSVGFNI+    V+F YMHH+ELP  +H GTDL G
Sbjct  120  GTVIGLYPVTMRSNGTIRASFLAGACGSVGFNIEKGVVNFFYMHHLELPNALHTGTDLMG  179

Query  180  NFYGPFVDRQTAQAAGTDTTITVNVLAWLYAAVI-------NGDRWFLNRFTTTLNDFNL  232
             FYG +VD + AQ    D  +T N++AWLYAA+I       +  +W L   T ++ D+N
Sbjct  180  EFYGGYVDEEVAQRVPPDNLVTNNIVAWLYAAIISVKESSFSQPKW-LESTTVSIEDYNR  238

Query  233  VAMKYNYEPLTQDHVDILGPLSAQTGIAVLDMCASLKELLQNGMNGRT--ILGSALLEDE  290
             A    + P +      +  LSA TG+   D+C  L+ ++       +  ILG    EDE
Sbjct  239  WASDNGFTPFSTSTA--ITKLSAITGV---DVCKLLRTIMVKSAQWGSDPILGQYNFEDE  293

Query  291  FTPFDVVRQCSGVTFQ  306
             TP  V  Q  GV  Q
Sbjct  294  LTPESVFNQVGGVRLQ  309
```

Fig. 8. Protein BLAST results of main proteases IBV and SARS-CoV-2

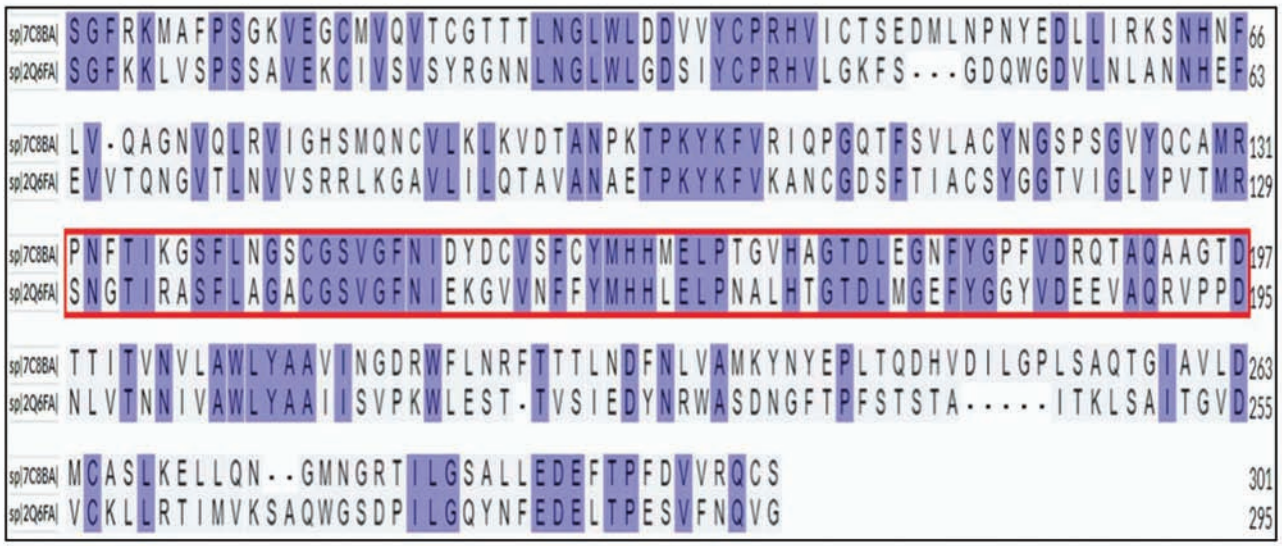

Fig. 9. The sequence alignment of main proteases of IBV (2Q6FA) and SARS-CoV-2 (7C8BA); red-active site of main protease (amino acids 130-190)

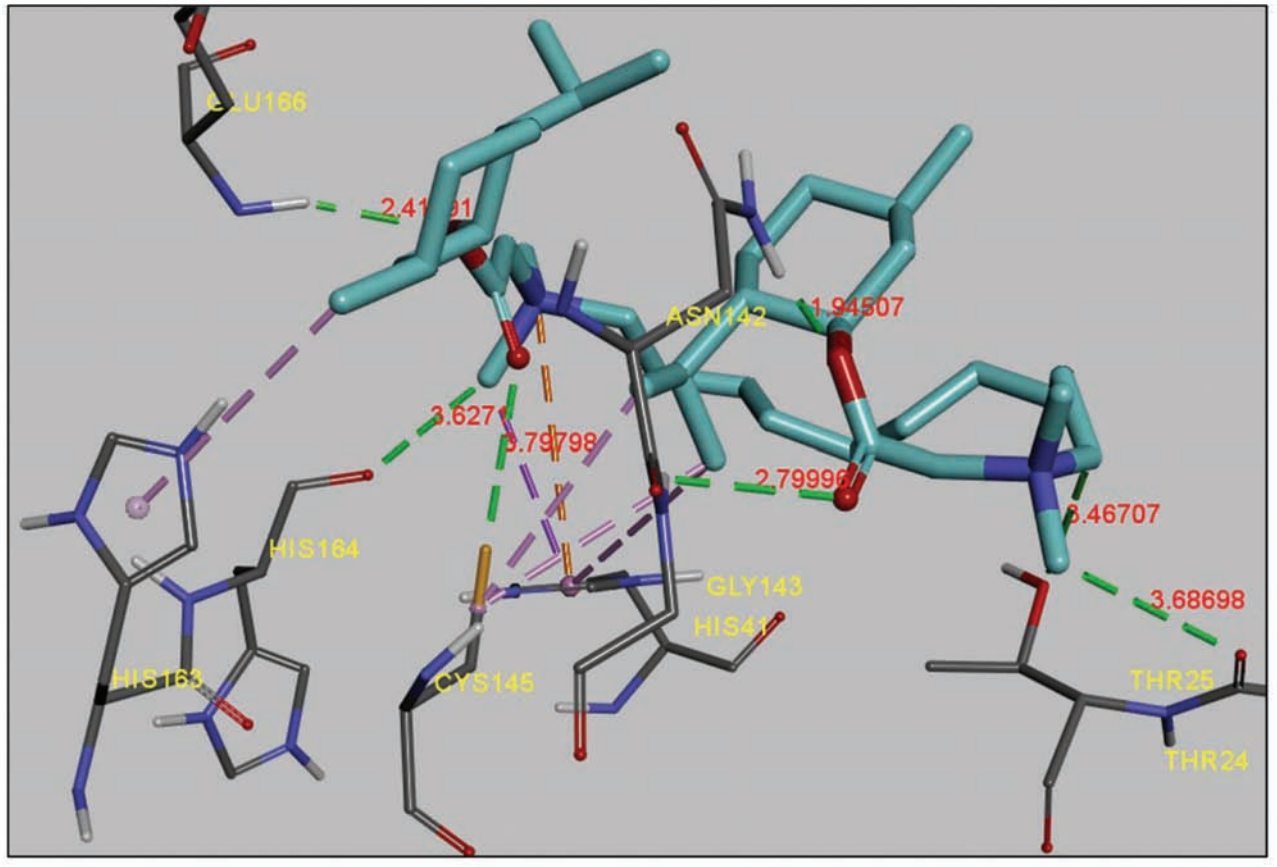

Fig. 10. Docking of decamethoxin into the SARS-CoV-2 M^{pro} active site

virucidal activity assessment of new disinfectants and antiseptics with a similar type of action against SARS-CoV-2.

Conflict of interest. Authors have completed the Unified Conflicts of Interest form at http://ukr-biochemjournal.org/wp-content/uploads/2018/12/coi_disclosure.pdf and declare no conflict of interest.

Funding. This work was supported by the National Academy of Sciences of Ukraine (No 0122U000837).

ОСОБЛИВОСТІ ВІРУЦИДНОЇ АКТИВНОСТІ ДЕКАМЕТОКСИНУ: ДОСЛІДЖЕННЯ *IN VITRO* ТА *IN SILICO*

І. В. Семенюта[1]✉, *О. П. Трохименко*[2], *І. В. Дзюблик*[2], *С. О. Соловйов*[2,3], *В. В. Трохимчук*[2], *О. Л. Боброва*[4], *Д. М. Година*[1], *М. П. Сметюх*[3], *О. К. Яковенко*[5], *Л. О. Метелиця*[1]

[1]Інститут біоорганічної хімії та нафтохімії ім. В. П. Кухаря НАН України, Київ;
[2]Національний університет охорони здоров'я України імені П.Л. Шупика, Київ, Україна;
[3]Національний технічний університет України «Київський політехнічний інститут імені Ігоря Сікорського», Київ;
[4]Національний інститут фтизіатрії і пульмонології ім. Ф. Г. Яновського НАМН України, Київ;
[5]Волинська обласна клінічна лікарня, Луцьк, Україна;
✉e-mail: ivan@bpci.kiev.ua

Наведено дані щодо короткочасної дії декаметоксину на штам H120 вірусу інфекційного бронхіту (IBV), який використовується як безпечна для людини модель вірусу SARS-CoV-2. Вірусну активність оцінювали за допомогою інвертованого мікроскопа PrimoVert (Німеччина) за деструктивною дією на лінію фібробластів BHK21. Результати *in vitro* показали, що декаметоксин (100 мкг/мл) повністю інактивував штам коронавірусу IBV при експозиції 30 с і більше. Під час найнижчої експозиції декаметоксину 10 сек антисептична віруліцидна активність становила 33 і 36% від контролю через 24 і 48 год культивування відповідно. Молекулярний докінг-аналіз вказав на значну подібність структури основної протеази (M^{pro}) IBV та SARS-CoV-2. Докінг-дослідження взаємодії декаметоксину з активними центрами IBV M^{pro} та SARS-CoV-2 M^{pro} продемонстрували утворення ліганд-протеїнових комплексів з орієнтовною енергією зв'язування -8,6, -8,4 ккал/моль та ключовими амінокислотними залишками ASN26, GLY141, GLU187, GLU164 , THR24, THR25, ASN142, GLY143, CYS145, HIS164 і GLU166.

Ключові слова: декаметоксин, четвертинні амонієві сполуки, віруцидна активність, штам IBV H120, SARS-CoV-2, основна протеаза, молекулярний докінг.

References

1. Chen N, Zhou M, Dong X, Qu J, Gong F, Han Y, Qiu Y, Wang J, Liu Y, Wei Y, Xia J, Yu T, Zhang X, Zhang L. Epidemiological and clinical characteristics of 99 cases of 2019 novel coronavirus pneumonia in Wuhan, China: a descriptive study. *Lancet*. 2020; 395(10223): 507-513.
2. van Doremalen N, Bushmaker T, Morris DH, Holbrook MG, Gamble A, Williamson BN, Tamin A, Harcourt JL, Thornburg NJ, Gerber SI, Lloyd-Smith JO, de Wit E, Munster VJ. Aerosol and Surface Stability of SARS-CoV-2 as Compared with SARS-CoV-1. *N Engl J Med*. 2020; 382(16): 1564-1567.
3. Rutala WA, Weber DJ. Disinfection, sterilization, and antisepsis: An overview. *Am J Infect Control*. 2019; 47S: A3-A9.
4. Choi A, Koch M, Wu K, Chu L, Ma L, Hill A, Nunna N, Huang W, Oestreicher J, Colpitts T, Bennett H, Legault H, Paila Y, Nestorova B, Ding B, Montefiori D, Pajon R, Miller JM, Leav B, Carfi A, McPhee R, Edwards DK. Safety and immunogenicity of SARS-CoV-2 variant mRNA vaccine boosters in healthy adults: an interim analysis. *Nat Med*. 2021; 27(11): 2025-2031.
5. Dhama K, Patel SK, Kumar R, Masand R, Rana J, Yatoo MI, Tiwari R, Sharun K, Mohapatra RK, Natesan S, Dhawan M, Ahmad T, Emran TB, Malik YS, Harapan H. The role of disinfectants and sanitizers during COVID-19 pandemic: advantages and deleterious effects on humans and the environment. *Environ Sci Pollut Res Int*. 2021; 28(26): 34211-34228.
6. Yoo JH. Review of disinfection and sterilization - back to the basics. *Infect Chemother*. 2018; 50(2): 101-109.

7. Kunduru KR, Kutner N, Nassar-Marjiya E, Shaheen-Mualim M, Rizik L, Farah S. Disinfectants role in the prevention of spreading the COVID-19 and other infectious diseases: The need for functional polymers! *Polym Adv Technol*. 2022; 10.1002/pat.5689.
8. Dan W, Gao J, Qi X, Wang J, Dai J. Antibacterial quaternary ammonium agents: Chemical diversity and biological mechanism. *Eur J Med Chem*. 2022; 243: 114765.
9. Wieczorek D, Dobrowolski A, Staszak K, Kwaśniewska D, Dubyk P. Synthesis, Surface and Antimicrobial Activity of Piperidine-Based Sulfobetaines. *J Surfactants Deterg.* 2017; 20(1): 151-158.
10. Dewey HM, Jones JM, Keating MR, Budhathoki-Uprety J. Increased use of disinfectants during the COVID-19 pandemic and its potential impacts on health and safety. *ACS Chem Health Saf*. 2021; 29(1); 27-38.
11. Gorbalenya AE, Baker SC, Baric RS, De Groot EJ, DrostenC, Gulyaeva AA, Haagmans BL, Lauber C, Leontovich AM, Neuman BW, Penzar D, Perlman S, Poon LLM, Samborskiy DV, Sidorov IA, Sola I, Ziebuhr J. The species Severe acute respiratory syndrome-related coronavirus: classifying 2019-nCoV and naming it SARS-CoV-2. *Nat Microbiol*. 2020; 5(4): 536-544.
12. Gerba CP. Quaternary ammonium biocides: efficacy in application. *Appl Environ Microbiol*. 2015; 81(2): 464-469.
13. Vereshchagin AN, Frolov NA, Egorova KS, Seitkalieva MM, Ananikov VP. Quaternary Ammonium Compounds (QACs) and Ionic Liquids (ILs) as Biocides: From Simple Antiseptics to Tunable Antimicrobials. *Int J Mol Sci*. 2021; 22(13): 6793.
14. Statistics of publications about QACs for 2021. Available at https://scholar.google.com/scholar?as_ylo=2021&q=quaternary+ammonium+compounds+&hl=en&as_sdt=0,5 (accessed, Yuli, 2022).
15. Huang Y, Xiao S, Song D, Yuan Z. Evaluating the virucidal activity of four disinfectants against SARS-CoV-2. *Am J Infect Control*. 2022; 50(3): 319-324.
16. Baker N, Williams AJ, Tropsha A, Ekins S. Repurposing Quaternary Ammonium Compounds as Potential Treatments for COVID-19. *Pharm Res.* 2020; 37(6): 104.
17. Schrank CL, Minbiole KPC, Wuest WM. Are Quaternary Ammonium Compounds, the Workhorse Disinfectants, Effective against Severe Acute Respiratory Syndrome-Coronavirus-2? *ACS Infect Dis.* 2020; 6(7): 1553-1557.
18. Halushko O. A clinical view on the possibility and feasibility of using decamethoxin during the COVID-19 pandemic. *Perioperaciina Medicina*. 2021; 4(1): 30-38.
19. Gumeniuk G, Gumeniuk M, Dziublik I, Fadeeva S, Opimakh S, Denysov O. The efficacy of the decamethoxin against simple and complex viruses. *Eur Respir J.* 2020; 56: 2388.
20. Attri P, Choi S, Kim M, Shiratani M, Cho AE, Lee W. Influence of alkyl chain substitution of ammonium ionic liquids on the activity and stability of tobacco etch virus protease. *Int J Biol Macromol*. 2020; 155: 439-446.
21. Bororova O. Efficacy and safety of decamethoxin in complex treatment of patients with group III viral-bacterial community-acquired pneumonia. *Infusion Chemotherapy.* 2021; (1): 15-21.
22. Cui J, Li F, Shi ZL. Origin and evolution of pathogenic coronaviruses. *Nat Rev Microbiol*. 2019; 17(3): 181-192.
23. Bharadwaj S, Azhar EI, Kamal MA, Bajrai LH, Dubey A, Jha K, Yadava U, Kang SG, Dwivedi VD. SARS-CoV-2 M pro inhibitors: identification of anti-SARS-CoV-2 M pro compounds from FDA approved drugs. *J Biomol Struct Dyn*. 2022; 40(6): 2769-2784.
24. Rut W, Groborz K, Zhang L, Sun X, Zmudzinski M, Pawlik B, Młynarski W, Hilgenfeld R, Drag M. Substrate specificity profiling of SARS-CoV-2 main protease enables design of activity-based probes for patient-sample imaging. *bioRxiv*. 2020.
25. Ullrich S, Nitsche C. The SARS-CoV-2 main protease as drug target. *Bioorg Med Chem Lett*. 2020; 30(17): 127377.
26. Ma C, Sacco MD, Hurst B, Townsend JA, Hu Y, Szeto T, Zhang X, Tarbet B, Marty MT, Chen Y, Wang J. Boceprevir, GC-376, and calpain inhibitors II, XII inhibit SARS-CoV-2 viral replication by targeting the viral main protease. *Cell Res.* 2020; 30(8): 678-692.
27. Sethi A, Joshi K, Sasikala K, Alvala M. Molecular docking in modern drug discovery: Principles and recent applications. Drug Discovery and Development-new advances. 2019; 2;2; 1-21.

28. Phillips MA, Stewart MA, Woodling DL, Xie ZR. Has molecular docking ever brought us a medicine? *Mol Docking.* 2018; 141.
29. Panwar U, Chandra I, Selvaraj C, Singh SK. Current Computational Approaches for the Development of Anti-HIV Inhibitors: An Overview. *Curr Pharm Des.* 2019; 25(31): 3390-3405.
30. Khan MA, Mahmud S, Alam ASMRU, Rahman ME, Ahmed F, Rahmatullah M. Comparative molecular investigation of the potential inhibitors against SARS-CoV-2 main protease: a molecular docking study. *J Biomol Struct Dyn.* 2021; 39(16): 6317-6323.
31. M Najimudeen S, H Hassan MS, C CorkS Abdul-Careem MF. Infectious Bronchitis Coronavirus Infection in Chickens: Multiple System Disease with Immune Suppression. *Pathogens.* 2020; 9(10): 779.
32. Crystal structure of the IBV main protease. (2022). Retrieved from https://www.rcsb.org/structure/2Q6F.
33. Crystal structure of the SARS-CoV-2 main protease. (2020). Retrieved from https://www.rcsb.org/structure/7L0D.
34. Sanner MF. Python: a programming language for software integration and development. *J Mol Graph Model.* 1999; 17(1): 57-61.
35. Marvin Sketch was used for drawing, displaying and optimization chemical structures, Marvin Sketch 5.3.735, 2022, ChemAxon (https://www.chemaxon.com).
36. MOPAC2016, James J. P. Stewart, Stewart Computational Chemistry, Colorado Springs, CO, USA, http://OpenMOPAC.net (2022).
37. Trott O, Olson AJ. AutoDock Vina: improving the speed and accuracy of docking with a new scoring function, efficient optimization, and multithreading. *J Comput Chem.* 2010; 31(2): 455-461.
38. Dassault Systèmes BIOVIA. Discovery Studio Visualizer, v4.0.100.13345. San Diego: Dassault Systèmes; 2022.
39. Xue X, Yu H, Yang H, Xue F, Wu Z, Shen W, Li J, Zhou Z, Ding Y, Zhao Q, Zhang XC, Liao M, Bartlam M, Rao Z. Structures of two coronavirus main proteases: implications for substrate binding and antiviral drug design. *J Virol.* 2008; 82(5): 2515-2527.
40. Dzyublik IV, Trokhimenko OP, Soloviov SO, Trokhymchuk VV, Bororova OL, Yakovenko OK. Efficacy decametoxin *in vitro* for quick inactivation of respiratory coronavirus. *Farmatsevt Zhurn.* 2022; 25(2); 87-101. (In Ukrainian).
41. Crystal structure of the SARS-CoV-2 main protease. (2020). Retrieved from https://www.rcsb.org/structure/ 7C8B.
42. Altschul SF, Gish W, Miller W, Myers EW, Lipman DJ. Basic local alignment search tool. *J Mol Biol.* 1990; 215(3): 403-410.
43. Pundir S, Martin MJ, O'Donovan C, UniProt Consortium. UniProt Tools. *Curr Protoc Bioinformatics.* 2016; 53: 1.29.1-1.29.15.